

Structural equation modelling reveals factors regulating surface sediment organic carbon content and CO₂ efflux in a subtropical mangrove

Author

Ouyang, Xiaoguang, Lee, Shing Yip, Connolly, Rod M

Published

2017

Journal Title

Science of the Total Environment

DOI

[10.1016/j.scitotenv.2016.10.218](https://doi.org/10.1016/j.scitotenv.2016.10.218)

Rights statement

© 2017 Elsevier. Licensed under the Creative Commons Attribution-NonCommercial-NoDerivatives 4.0 International (<http://creativecommons.org/licenses/by-nc-nd/4.0/>) which permits unrestricted, non-commercial use, distribution and reproduction in any medium, providing that the work is properly cited.

Downloaded from

<http://hdl.handle.net/10072/343364>

Griffith Research Online

<https://research-repository.griffith.edu.au>

Structural equation modelling reveals factors regulating surface sediment organic carbon content and CO₂ efflux in a subtropical mangrove

Xiaoguang Ouyang, Shing Yip Lee, Rod M. Connolly

Australian Rivers Institute – Estuaries and Coast, and School of Environment, Griffith University, Gold Coast, Queensland 4222, Australia

Email: oyxiaoguang@gmail.com

Corresponding author: Xiaoguang Ouyang

Citation: Ouyang, X., Lee, S.Y., Connolly, R.M. (2017) Structural equation modelling reveals factors regulating sediment carbon stock and CO₂ flux in subtropical mangroves. *Science of the Total Environment*, 578: 513-522. doi: 10.1016/j.scitotenv.2016.10.218.

Abstract

Mangroves are blue carbon ecosystems that sequester significant carbon but release CO₂, and to a lesser extent CH₄, from the sediment through oxidation of organic carbon or from overlying water when flooded. Previous studies, e.g. Leopold et al. (2015), have investigated sediment organic carbon (SOC) content and CO₂ flux separately, but could not provide a holistic perspective for both components of blue carbon. Based on field data from a mangrove in southeast Queensland, Australia, we used a structural equation model to elucidate (1) the biotic and abiotic drivers of surface SOC (10 cm) and sediment CO₂ flux; (2) the effect of SOC on sediment CO₂ flux; and (3) the covariation among the environmental drivers assessed. Sediment water content, the percentage of fine-grained sediment (<63µm), surface sediment chlorophyll and light condition collectively drive sediment CO₂ flux, explaining 41% of their variation. Sediment water content, the percentage of fine sediment, season, landform setting, mangrove species, sediment salinity and chlorophyll collectively drive surface SOC, explaining 93% of its variance. Sediment water content and the percentage of fine sediment have a negative impact on sediment CO₂ flux but a positive effect on surface SOC content, while sediment chlorophyll is a positive driver of both. Surface SOC was significantly higher in *Avicennia marina* (2994±186 g m⁻², mean±SD) than in *Rhizophora stylosa* (2383±209 g m⁻²). SOC was significantly higher in winter (2771±192 g m⁻²) than in summer (2599±211 g m⁻²). SOC significantly increased from creek-side (865±89 g m⁻²) through mid (3298±137 g m⁻²) to landward (3933±138g m⁻²) locations. Sediment salinity was a positive driver of SOC. Sediment CO₂ flux without the influence of biogenic structures (crab burrows, aerial roots) averaged 15.4 mmol m⁻² d⁻¹ in *A. marina* stands under dark conditions, lower than the global average dark flux (61 mmol m⁻² d⁻¹) for mangroves.

Keywords: mangroves, sediment, blue carbon, SOC content, CO₂ flux, structural equation model

1 Introduction

Mangroves are intertidal ecosystems with high carbon (C) sequestration capacity (Bouillon et al., 2008) as well as C stock in sediment (Adame et al., 2013; Brown et al., 2016; Donato et al., 2011; Friess et al., 2015). Mangrove sediment biogeochemistry is complex and variable, and responds to both biotic and abiotic drivers. Mangrove organic material such as leaf litter, if not exported, enters the sediment and, along with roots are decomposed by microbes (e.g. bacteria) (Kristensen et al., 2008a). CO₂ is the main gas product of sediment OC oxidation as methanogenesis is considered to be a minor process in marine sediments (Penha-Lopes et al., 2010).

Carbon stocks in mangroves consist of C of above- and belowground vegetation, as well as sediment C; the latter is the focus of this study. Sediment organic C (SOC) stock in mangroves has been shown to be regulated by different environmental factors in different studies (Alongi, 2014). For example, SOC stock was found to vary with sediment salinity, and-nutrient content (e.g. N and P) in a Mexican mangrove (Adame et al., 2013). SOC stock can be widely different among mangrove species – a comparison among *Laguncularia racemosa*, *Rhizophora mangle* and *Conocarpus erectus* resulted in a large range (23–190 kg m⁻²); and seasons and sediment types were proposed to be the most important drivers for SOC stock on Carmen Island, Mexico (Cerón-Bretón et al., 2014). It was also reported that SOC stock changes along the transect from the seaward, through interior, to landward sites (Kauffman et al., 2011). Sediment microphytobenthos are also considered to be a significant source of C in mangrove sediments, second to C fixed from the air by the trees (Alongi, 2014).

In addition to the factors that modulate SOC stock, biogenic structures (such as crab burrows and aerial roots) and light conditions are the external drivers of sediment CO₂ flux. Although biogenic structures are directly related to the microphytobenthos, they also promote sediment CO₂ flux via other processes, e.g. increasing the area of sediment and air/water interfaces by epibenthic burrows (Lee, 2008). Likewise, light conditions are directly related to the microphytobenthos but primarily affect CO₂ assimilation during photosynthetic processes. Further, OC content in sediment and bulk density, and thus SOC, account for variations in sediment CO₂ flux (Chen et al., 2010). Pneumatophores and animal burrows can promote sediment CO₂ emission in *Sonneratia alba* and *Avicennia marina* forests (Kristensen et al., 2008b). Sediment CO₂ flux under light conditions may be generally low compared to the dark flux, due to CO₂ uptake by the microphytobenthos during photosynthesis (Bouillon et al., 2008). Sediment CO₂ flux was also shown to vary along the sea-land gradient and with

sediment properties (Chen et al., 2010) and mangrove species, as well as chlorophyll a (Chl a) (Leopold et al., 2013) and seasons (Chen et al., 2012) in mangroves.

Despite numerous studies examining the factors that independently influence SOC stock and CO₂ flux, the relationships among SOC stock, sediment CO₂ flux and their drivers have not been analysed in one comprehensive model. It is important to explore the relationships in a single analysis because identifying the relative weight of drivers of both SOC stock and sediment CO₂ flux would provide insights into effective blue C management (McLeod et al., 2011). SOC stock is not only a response variable dependent on sediment physico–chemical properties, landform settings, seasons and species, but also a potential predictor for sediment CO₂ flux. Soil CO₂ flux measured by the chamber technique accounts for CO₂ from the soil surface (Alongi, 2014), and thus surface SOC is utilised as the specific predictor for sediment CO₂ flux measured in our study. It is also of interest directly as well, as to what environmental variables relate to surface SOC. For sediment CO₂ flux, in addition to the same influential factors that regulate SOC stock, the drivers may also include sediment temperature, light conditions and biogenic structures (Kristensen & Alongi, 2006). Additionally, some factors exert influences on each other, this redundancy may be reflected in an overall model. Structural equation modelling is a statistical method capable of resolving this type of problem: (1) when the indirect effects of one predictor influence a second predictor, which in turn influences the response variable; and (2) there exists two or more response variables which can interact with each other (Quinn & Keough, 2002).

In this study, based on data collected from a subtropical mangrove forest in southeast Queensland, Australia, structural equation modelling was used to evaluate (1) factors regulating sediment CO₂ flux, including surface SOC, sediment physico–chemical properties, landform settings, seasons, species, the density of biogenic structures and light conditions; (2) factors modulating surface SOC, including sediment physico–chemical properties, landform settings, seasons and species; and (3) possible correlations among the influential factors.

2 Materials and methods

2.1 Conceptual model

Based on the prior knowledge on factors influencing SOC stock and CO₂ flux, a conceptual model was established (Fig. 1). From reported studies, the common factors affecting both

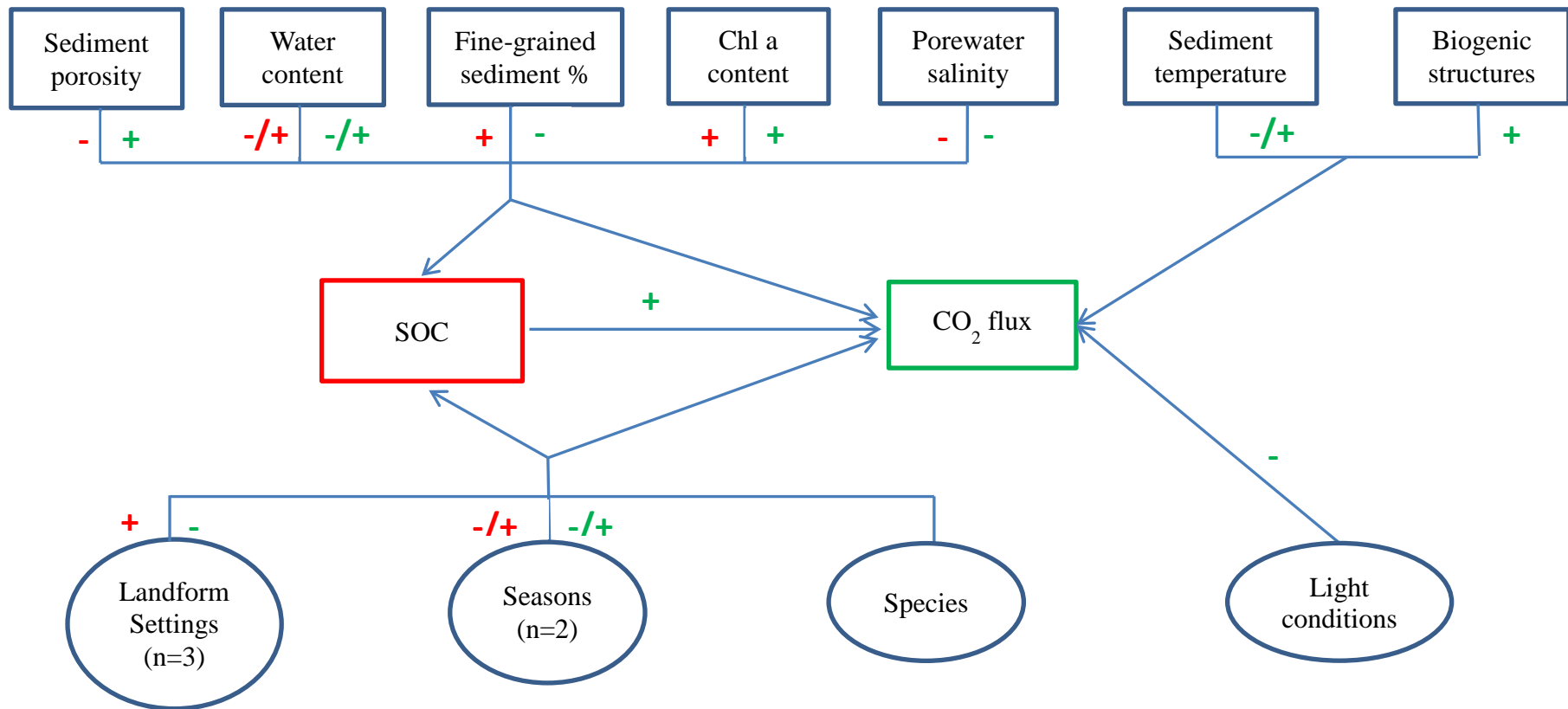


Fig. 1 Influential drivers of sediment surface SOC stock and sediment CO₂ flux identified based on priori analysis. Green and red colours are used to denote the influence of factors on surface SOC and sediment CO₂ flux, respectively. Positive and negative effects are denoted by + and -, respectively. Qualitative variables were quantified in Section 2.5 'Statistical analysis'. Species in studies reviewed are different from those in this study, and thus no specific effects were shown.

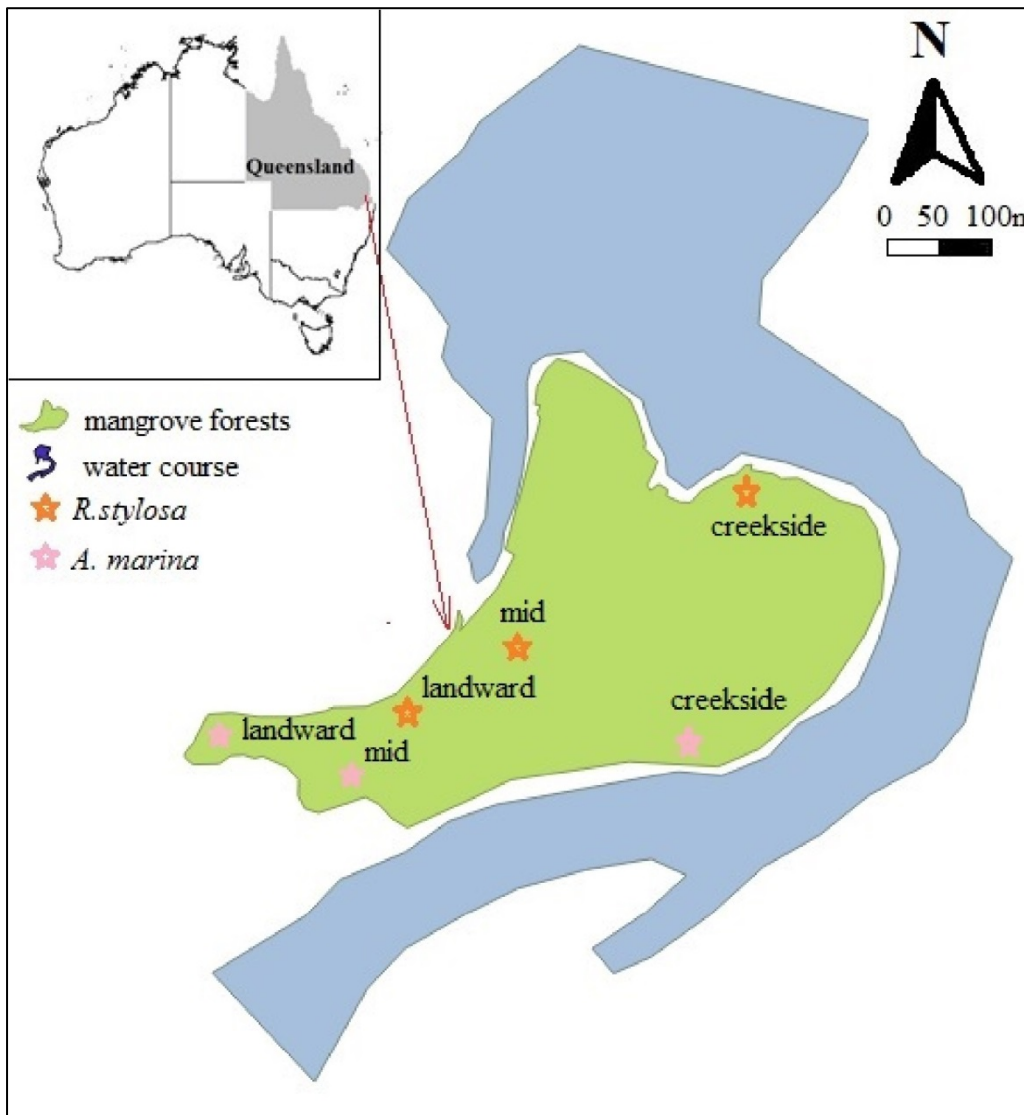


Fig. 2 The sampling location ($28^{\circ}6'28.8''S$, $153^{\circ}26'48.72''E$) in Southeast Queensland, Australia. The coordinates of the transects are as below: (1) *A. marina* (creekside: $28^{\circ}6'32.85''S$, $153^{\circ}26'53.56''E$, mid: $28^{\circ}6'33.48''S$, $153^{\circ}26'44.21''E$, landward: $28^{\circ}6'33.23''S$, $153^{\circ}26'39.74''E$), (2) *R. stylosa* (creekside: $28^{\circ}6'26.65''S$, $153^{\circ}26'53.84''E$, mid: $28^{\circ}6'30.38''S$, $153^{\circ}26'47.35''E$, landward: $28^{\circ}6'32.15''S$, $153^{\circ}26'45.06''E$).

SOC stock and CO₂ flux in mangroves include, but not limited to, sediment particle size, gravitational/volumetric water content, sediment porosity, Chl a, seasons, landform settings, species and porewater salinity. Sediment CO₂ flux is also affected by SOC stock and potentially by an array of other factors, i.e. sediment temperature, the densities of pneumatophores and burrows, as well as light conditions (dark or light). Sediments were categorized into gravel, sand, silt and clay particle size classes according to the Udden scale. The aggregated proportion of silt and clay was used to consider the influence of silt and clay particles.

2.2 Sampling site

The sampling site is located in a mangrove forest, along Tallebudgera Creek, southeast Queensland, Australia (Fig. 2). The forest is dominated by *A. marina* and *Rhizophora stylosa*. According to climate records from the nearest weather station at Coolangatta 8 km away from the sampling site, average annual rainfall is 1507.5 mm and average temperature is 24.7 °C (<http://www.bom.gov.au/>). The climate at the sampling site generally comprises a cool dry winter and hot wet summer. Average temperature is 21.9 °C in winter between May and September, but 25.3 °C in summer (October–April). The mangroves experience diurnal tides. According to tidal records from the nearest tidal gauge (Gold Coast Operations Base) 15 km from the sampling site, heights of high tides range from 0.9–1.86 m in summer and 0.94–1.92 m in winter, while heights of low tides range from 0–0.62 m in summer and 0–0.65 m in winter.

2.3 Sampling campaign

Sediment CO₂ flux measurements were conducted in the cool (August 2015) and warm seasons (January 2016) at three locations along a transect from the creekside towards the landward extreme of the mangrove forest. The three locations represent increasing distances from the creek. Sediment physico-chemical properties (e.g. salinity) and crab burrow densities are distinct along the transect. Elevations of the locations are similar (difference within 10 cm). At each location, sediment CO₂ flux was measured 2 h before high tide at five replicate points (~3 m on average distance between each replicate) each in the *A. marina* and *R. stylosa* forests. The measurements were conducted either in shaded or in sunlight exposed areas, depending on vegetation cover. Both dark and light fluxes were measured, with opaque and transparent chambers made of polycarbonate (custom built model), respectively. 60 measurements of sediment CO₂ flux was conducted in each season, i.e., 120 measurements in

the whole survey. Sediment CO₂ flux from the sediment–air interface has been measured to represent flux from all the contributors. The removal of surface microbial mat will modify sediment profiles, change the oxygen distribution and anoxic–oxic interface and result in increasing diffusion gradients. It still remains unknown what is the duration of the biofilm removal effect (Bulmer et al., 2015). Before sampling, the chambers were pushed into the sediment and remained so for 20 min. A SBA–5 gas analyser (PP systems, USA) was used to measure sediment CO₂ flux for around 2.5 min in a closed loop, including a chamber (volume = 5.7 L) and rotary pump (200 mL min⁻¹). The surface area of sediment covered by the chamber is 0.1 m². The short incubation period (2.5 min) was selected to avoid the variation of micro–climatic conditions under the chambers (Jensen et al., 1996; Kabwe et al., 2002). Zero calibration was conducted using a soda lime canister to scrub CO₂ down before each measurement. The operation was conducted following PP Systems (2012). Sediment CO₂ flux was calculated *as per* the following formula.

$$F = \frac{\left(\frac{\Delta C_{CO_2}}{\Delta t}\right)V}{RTA}$$

Where F is the sediment CO₂ flux, in $\mu\text{mol m}^{-2} \text{s}^{-1}$; C_{CO_2} is CO₂ concentration of the gases trapped in the closed loop and measured by the SBA–5 gas analyser (ppm); $\frac{\Delta C_{CO_2}}{\Delta t}$ is the variation of C_{CO_2} as a function of the measurement period (2.5 min) (ppm s⁻¹); V is the volume of the closed loop, which consists of a chamber plus pipes connecting the SBA–5 and the chamber (m³); R is the ideal gas constant of 8.20528 atm m³ K⁻¹ mol⁻¹; T is *in situ* air temperature measured by temperature sensors (K); A is the surface area of sediment covered by the chamber, 0.1 m².

Concurrent with the CO₂ flux measurement, sediment and air temperature was recorded by temperature sensors at each site. After each flux measurement, the numbers of crab burrows and pneumatophores were counted within each chamber. Only *A. marina* has pneumatophores, which are so extensive that can be observed in *R. stylosa*. Subsequently, the upper sediment layer was collected for Chl *a* analysis, a proxy for the abundance of microphytobenthos. Intact sediment samples (top 1 cm) were placed in a jar, covered with aluminium foil, avoiding mixing and transported in a cool box to the laboratory, always protected from light and high temperatures. Sediment to a depth of 10 cm was cored to provide samples for other physico–chemical analysis, including loss on ignition (LOI), bulk density, gravimetric and volumetric water content, porosity, sediment porewater salinity and

grain size. We never intended to measure all possible variables. For structural equation modelling, the minimum ratio of sample sizes/variables is 10:1 (Hoyle, 2012), which we achieved in our study by limiting the variables being examined to those deemed most important. If more variables were included, the ratio would have been <10:1 and not justified for the model in our study.

2.4 Sample analysis

On return to the laboratory, the sediment samples for Chl a analysis were hand-stirred thoroughly to ensure homogeneity and around 10 g homogenised sediments were sampled and put in plastic tubes, covered with aluminium foil. 90% aqueous acetone was added to each sample and the tubes were agitated by a MSI minishaker. The samples were then placed in a -20 °C freezer overnight. Before analysis, the tubes were centrifuged for 10 min at 3000 rpm, and then analysed for Chl a using a spectrophotometer (Shimadzu Corporation, Japan) following the procedure of Brito et al. (2009).

Other sediment samples were kept frozen before physico-chemical analysis. A set of sediment samples was dried at 80 °C for 48 h in a Thermotec 2000 oven, and analysed for bulk density, gravimetric and volumetric water content, and porosity. After acid treatment by 1 N HCl solution until effervescence stopped, the C content of the sediment was estimated using the LOI method. The dry sediment was combusted in a muffle furnace (Lenton thermal designs, UK) at 550 °C for 4 h. OC content in sediment was estimated from LOI by dividing the % weight loss by 1.73 (Schumacher, 2002). Sediment porewater salinity was analysed by adding MilliQ water to dried sediment samples, stirring the samples and then the salinity of the water was determined by a refractometer (Master series, ATAGO, Japan) (Douglas & McConchie, 1994). The distribution of sediment grain sizes was analysed by the wet sieving method with a series of sieves, i.e. 63 µm and 2000 µm, thus separated the sediment to different grains: silt and clay (<63 µm), sand (63–2000 µm) and gravel (>2000 µm).

2.5 Statistical analysis

Structural equation modelling was used to analyse the data. It is a method that can be used when multivariate normality is not met (Schumacker and Lomax, 2004). The relationship between surface SOC content or sediment CO₂ flux and influential factors was defined by linear regression. In total, 14 variables were involved in the initial model. In addition to the regression model, the error covariance of sediment CO₂ flux and surface SOC was considered in the structural equation model to control error correlation. The sample size (120) is larger

than 100, which has been suggested as the minimum samples for the structural equation model by Schumacker and Lomax (2004). Table 1 shows the variables included in the model.

Table 1 Variables included in the initial and final structural equation models. Dependent variables were sediment surface SOC content and sediment CO₂ flux

Independent variables	Explanatory variables for surface SOC content or sediment CO ₂ flux?	
	As independent variable in the initial model for:	As independent variable in the final model for:
Sediment water content	Both	Both
Sediment porosity	Both	Sediment CO ₂ flux (NS)
Proportion of silt and clay	Both	Both
Crab burrow density	Both	Sediment CO ₂ flux (NS)
Pneumatophore density	Sediment CO ₂ flux	Neither
Sediment temperature	Sediment CO ₂ flux	Neither
Sediment Chl a	Both	Both
Porewater salinity	Both	surface SOC content
Landform settings	Both	surface SOC content
Seasons	Both	surface SOC content
Species	Both	Sediment CO ₂ flux (NS), surface SOC content
Light condition	Sediment CO ₂ flux	Sediment CO ₂ flux

NS denotes not significant.

Before modelling, data exploration was undertaken between surface SOC content or sediment CO₂ flux and individual factors, and significant outliers were removed. Overall, five outliers were removed before analysis. For example, one datum within the whole data set on the percentage of fine-grain sediment is 97.1%, and is a significant outlier since it greatly deviates from the others in the whole data set, which have a range of 1.1–73.3%. Data were then checked for univariate and multivariate normality, and multivariate outliers. As for multivariate outlier checking, factors were removed if variance inflation factors (VIF) were > 10. As the assumption of multivariate normality could not be met, the Bollen–Stine bootstrap

was used since it can provide the correct p-values ($\alpha = 0.05$) for the chi-square statistic to evaluate the overall model fit (null hypothesis: the best model is not different from the null model if $p < 0.05$). Significant interactions of independent variables were included in the initial model, but were finally excluded due to multivariate outliers. Bootstrap standard errors were calculated using model-based bootstrapping. The number of bootstrap draws was set as 400, which is larger than that suggested by Hoyle (2012). Surface SOC content and sediment CO₂ flux were square-root or third-root transformed to rescale the variables to the same levels as other influential factors. Landform settings, seasons, light conditions and species are ordinal variables, and were relevelled. The landform settings have three levels: creekside (0), middle (1) and landward (2). Seasons have two levels summer (0) and winter (1). The light conditions have two levels: dark (0) and light (1). The species have two levels: *A. marina* (0) and *R. stylosa* (1).

A variety of indices was used to evaluate the model fit, including the Comparative Fit Index (CFI), root mean square error of approximation (RMSEA) and Tucker-Lewis Index (TLI). The criteria for good fit of the above indices are: $CFI \geq 0.95$, $TLI \geq 0.95$ and $RMSEA \leq 0.05$. The non-significant factors were dropped from the model in case the original model could not meet the criteria, and this step continued until the model fit was reached. When quantitative independent variables were correlated with ordinal independent variables, the differences in quantitative independent variables were further explored. For ordinal variables with three levels, the Kruskal-Wallis rank sum test was conducted, followed by the Mann-Whitney test if there was a significant treatment effect. The same procedure was run for ordinal variables that are significant estimates for surface SOC content or sediment CO₂ flux in the structural equation model. Linear regression was performed between sediment CO₂ flux under dark conditions and the densities of crab burrows and pneumatophores.

R programming language (R Core Team, 2014) was used to conduct data analysis. The R packages 'car' (Fox & Weisberg, 2011), 'lavaan' (Rosseel, 2012), 'MVN' (Korkmaz S et al., 2014) and 'psych' (Revelle, 2015) were used to conduct assumption checking and structural equation modelling. 'semPlot' (Epskamp, 2014) was used to plot the structure equation model.

3 Results

3.1 Drivers of sediment CO₂ flux and surface SOC variation

Both components of blue carbon show spatial and seasonal changes, and vary with species. Sediment CO₂ flux was found to increase with seasons changing from winter ($184 \pm 34 \text{ mmol m}^{-2} \text{ d}^{-1}$, mean \pm SD) to summer ($313 \pm 46 \text{ mmol m}^{-2} \text{ d}^{-1}$), whereas surface SOC content shows the opposite trend, higher in winter ($2771 \pm 192 \text{ g m}^{-2}$) than in summer ($2599 \pm 211 \text{ g m}^{-2}$). Similarly, sediment CO₂ flux was higher, while surface SOC was lower, in *R. stylosa* (flux $310 \pm 45 \text{ mmol m}^{-2} \text{ d}^{-1}$, SOC $2383 \pm 209 \text{ g m}^{-2}$) than in *A. marina* (flux $182 \pm 35 \text{ mmol m}^{-2} \text{ d}^{-1}$, SOC $2993 \pm 186 \text{ g m}^{-2}$) stands. Sediment CO₂ flux was higher at creekside locations ($306 \pm 64 \text{ mmol m}^{-2} \text{ d}^{-1}$) than at mid ($200 \pm 45 \text{ mmol m}^{-2} \text{ d}^{-1}$) and landward locations ($232 \pm 37 \text{ mmol m}^{-2} \text{ d}^{-1}$), while surface SOC content was a magnitude lower at creekside locations ($865 \pm 89 \text{ g m}^{-2}$) than at mid ($3298 \pm 137 \text{ g m}^{-2}$) and landward locations ($3933 \pm 138 \text{ g m}^{-2}$) (Table 2, Fig. 3).

The structural equation model (see Fig. 4) has a close model–data fit (test statistic = 7.57, df = 8, p (Bollen–Stine Bootstrap) = 0.603). Sediment water content, the proportion of silt and clay, Chl a and light condition were significant drivers of sediment CO₂ flux, explaining 41% of its variation ($R^2 = 0.41$). Sediment water content, the proportion of silt and clay, seasons, landform settings, mangrove species, salinity and Chl a were significant drivers of surface SOC content, explaining 93% of its variance ($R^2 = 0.93$).

More specifically, as common estimates of both sediment CO₂ flux and surface SOC, water content and the proportion of silt and clay have a negative influence (the partial effect $r_{\alpha} = -0.036$ and -0.08) on sediment CO₂ flux but a positive influence ($r_{\alpha} = 0.414$ and 0.204) on surface SOC content. In contrast, sediment Chl a has a positive effect on both sediment CO₂ flux ($r_{\alpha} = 0.043$) and surface SOC ($r_{\alpha} = 0.273$). Furthermore, light condition was the exclusive estimate for sediment CO₂ flux, and the change from dark to light conditions resulted in a reduction in flux ($r_{\alpha} = -4.756$, Fig. 3). Surface SOC content was also regulated by external factors, including seasons, landform settings, mangrove species and sediment salinity. Among the external estimates, surface SOC content increased with seasons changing from summer to winter ($r_{\alpha} = 8.491$, Fig. 3) but decreased with species shifting from *A. marina* to *R. stylosa* ($r_{\alpha} = -3.531$, Fig. 3). Surface SOC content was also significantly different among landform settings ($\chi^2(2) = 80.2$, $p < 0.001$), and in particular, increasing along the transect from creekside through mid to landward locations (Mann–Whitney test, $p < 0.01$, Fig. 3). Surface SOC content was positively correlated with sediment salinity ($r_{\alpha} = 0.186$).

3.2 Interrelationships among influential factors

Table 2 Spatio-temporal variation of sediment CO₂ flux, surface SOC, densities of biogenic structures and sediment physico-chemical properties (mean ± standard error).

Variable	Landform settings			Seasons		Species	
	Creekside (n = 40)	Mid (n = 40)	Landward (n = 40)	Summer (n = 60)	Winter (n = 60)	<i>A. marina</i> (n = 60)	<i>R. stylosa</i> (n = 60)
Sediment CO ₂ flux (mmol m ⁻² d ⁻¹)	306 ± 64	200 ± 45	232 ± 37	313 ± 46	184 ± 34	182 ± 35	310 ± 45
Surface SOC (g m ⁻²)	865 ± 89	3298 ± 137	3933 ± 138	2599 ± 211	2771 ± 192	2993 ± 186	2383 ± 209
Pneumatophore density (m ⁻²)	33.8 ± 10.6	76.7 ± 13.5	42.4 ± 12.5	67.5 ± 12.1	35.7 ± 7.7	55.2 ± 4.6	46 ± 10.5
Crab burrow density (m ⁻²)	5.9 ± 1.4	50.5 ± 9.5	19.4 ± 3.8	38 ± 7.2	13.5 ± 2.5	33.4 ± 7.8	15.2 ± 2.8
Sediment porewater salinity (‰)	3.7 ± 0.4	13.5 ± 1.2	18.6 ± 2.4	6 ± 0.5	17.3 ± 1.7	13.9 ± 1.7	9.9 ± 1.2
Gravitational water content, %	18.2 ± 1.6	64.9 ± 2.9	99.1 ± 7.2	54.2 ± 4.7	66.1 ± 6.4	67.5 ± 5.9	53.2 ± 5.4
Volumetric water content (%)	19.9 ± 1.8	58.8 ± 1.9	62.1 ± 1.5	47.3 ± 2.8	46.3 ± 3	50.3 ± 2.3	43.3 ± 3.4
The percentage of fine-grained sediment (%)	12.6 ± 2.1	14.3 ± 1.1	13.5 ± 1.3	14.6 ± 0.9	12.4 ± 1.5	14.6 ± 1.4	12.3 ± 1.1
Porosity (%)	59.4 ± 0.7	64.9 ± 0.8	72.4 ± 1.6	64 ± 0.9	66.9 ± 1.3	66 ± 1.3	65 ± 0.9
Chl a (µg L ⁻¹)	494 ± 75	1508 ± 251	906 ± 121	1790 ± 149	205 ± 20	988 ± 163	952 ± 129

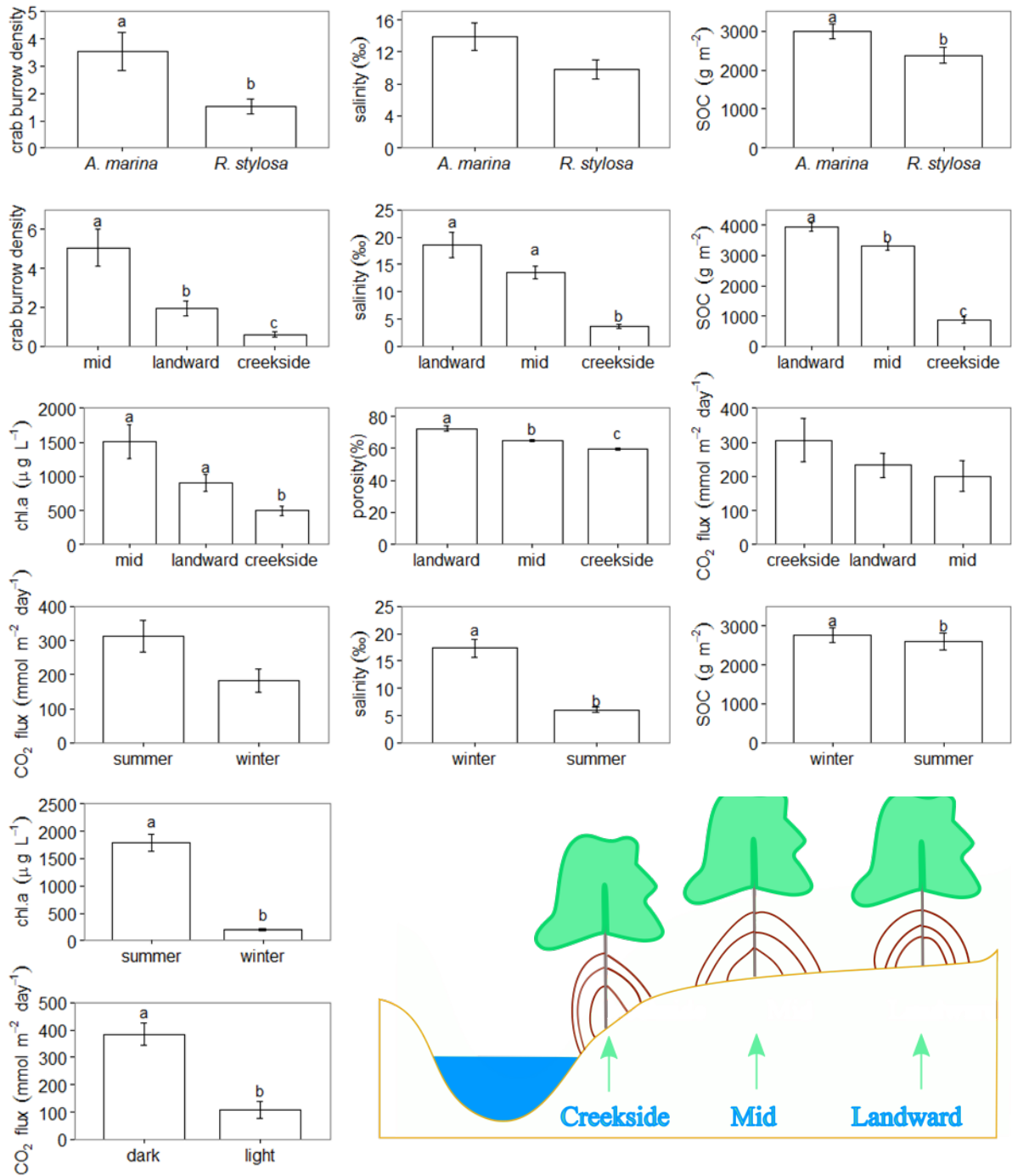


Fig. 3 The difference in sediment CO₂ flux, surface SOC content and physico-chemical properties among seasons, species, light conditions and landform settings. Error bars labelled with different letters were significantly different with each other. For clarity, only *Rhizophora* is illustrated in the inset on position of the mangrove stands along the creek-land transect.

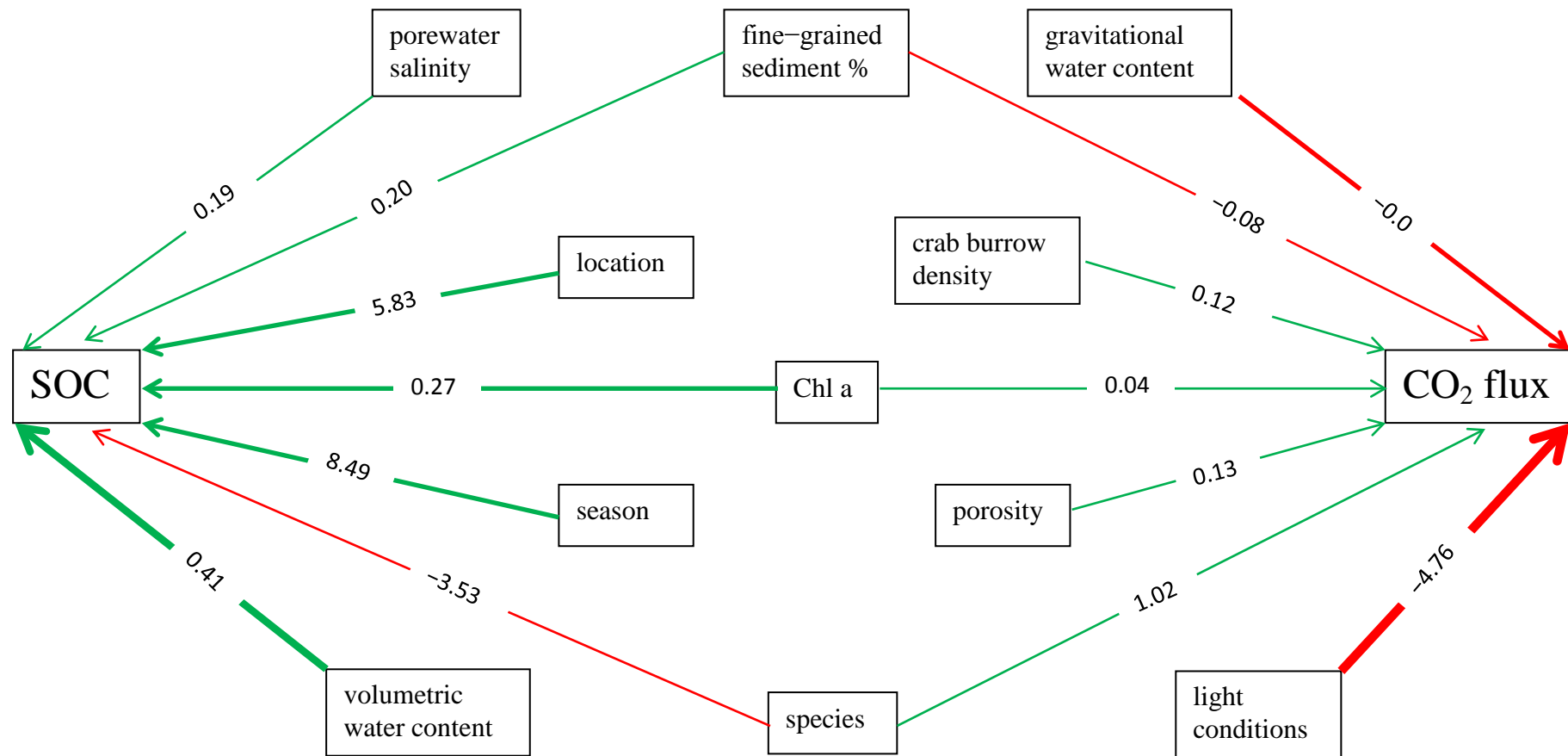


Fig. 4 The final structural equation model. Green and red colours indicate positive and negative estimates, respectively. Numbers in the figure represent each estimate of explanatory variables for SOC or CO₂ flux. The width of the arrows indicates the importance of each estimate.

Biotic and abiotic drivers of sediment CO₂ flux and surface SOC also show spatio-temporal variation (Table 2). Chl a, pneumatophore and crab burrow densities decreased along the transect from mid through landward to creekside locations, and seasonal transition from summer to winter. In contrast, sediment porewater salinity, gravitational/volumetric water content and porosity increased with increasing distances to the creek, and with seasonal transition from summer to winter except volumetric water content.

The possible correlations among influential variables for sediment CO₂ flux and surface SOC were further explored in the structural equation model (Table 3). The density of crab burrows was positively correlated with sediment volumetric water content (R = 0.25) and Chl a (R = 0.64). Sediment Chl a had a negative correlation with salinity (R = -0.27). Sediment porosity had a positive correlation with both sediment volumetric water content (R = 0.42) and salinity (R = 0.73), and a stronger correlation was found between sediment gravimetric water content and porosity (R = 0.85). The proportion of silt and clay was positively correlated with sediment volumetric water content (R = 0.23).

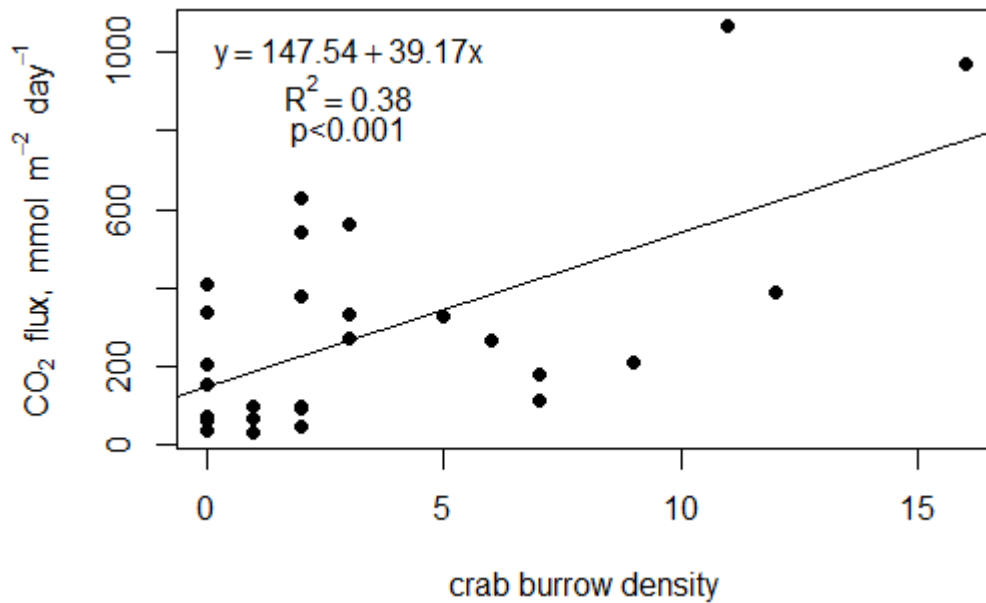
Table 3 Correlation among predictors in the structural equation model. Only significant pairs are included.

Effect	R
Gravimetric water content ~ sediment porosity	0.85
Proportion of silt and clay ~ sediment volumetric water content	0.23
Density of crab burrows ~ sediment Chl a	0.64
Density of crab burrows ~ sediment volumetric water content	0.25
Sediment Chl a ~ sediment salinity	-0.27
Sediment porosity ~ sediment volumetric water content	0.42
Sediment porosity ~ sediment salinity	0.73

Moreover, the density of crab burrows was found to decrease shifting from *A. marina* to *R. stylosa* ($r_a = -0.509$, Fig. 3). Sediment salinity increased, while Chl a decreased, as seasons changed from summer to winter ($r_a = 2.831$ and -6.86 , Fig. 3). The density of crab burrows, sediment Chl a, salinity and porosity varied with landform settings ($\chi^2(2) = 30.6, 17.8, 47.4$ and $40.6, p < 0.001$, Fig. 3). Further exploration indicated that sediment porosity and salinity generally increased along the transect from creekside through mid to landward locations (Mann-Whitney test, $p < 0.001$), except for the non-significant difference of

sediment salinity between the mid and landward sites (Mann–Whitney test, $p > 0.05$). The density of crab burrows and sediment Chl a generally decreased in the sequence of mid, landward and creekside locations (Mann–Whitney test, $p < 0.01$), except for the insignificant difference of sediment Chl a between the mid and landward sites (Mann–Whitney test, $p > 0.05$).

a)



b)

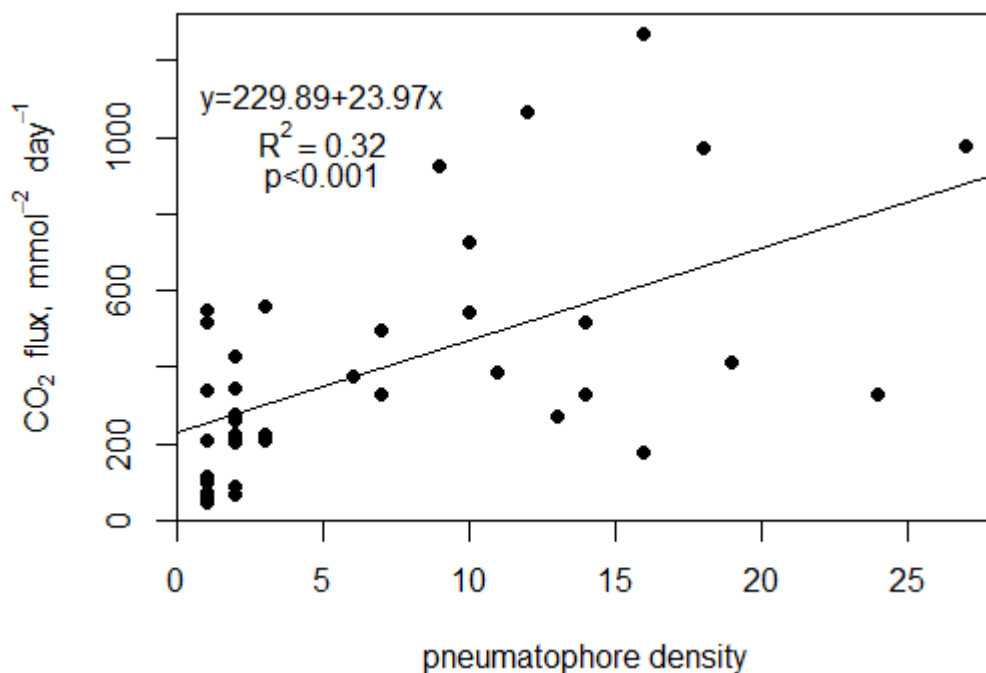


Fig. 5 The relationship between sediment CO_2 flux under dark conditions and the density of (a) crab burrows and (b) pneumatophores in *A. marina* forests.

3.3 Sediment CO₂ flux without the influence of biogenic structures

There are significant relationships between sediment CO₂ flux (including biogenic structures) and the densities of crab burrows ($R^2 = 0.38$, $p < 0.001$) as well as pneumatophores ($R^2 = 0.32$, $p < 0.001$) for *A. marina* (Fig. 5), while no significant relationships were found for *R. stylosa* ($p > 0.05$). Therefore, sediment CO₂ flux in *R. stylosa* forests, in the absence of biogenic structures, cannot be estimated since no statistically significant relationship is found between our measured sediment CO₂ flux and the densities of biogenic structures. Only results on *A. marina* are therefore reported here.

Based on the dark sediment flux data and statistically significant relationships stated above, sediment CO₂ flux = $148 + 39.2 * \text{crab burrow density}$, and sediment CO₂ flux = $230 + 24.0 * \text{pneumatophore density}$. Dark sediment CO₂ flux averaged $279 \text{ mmol m}^{-2} \text{ d}^{-1}$ in *A. marina* forests. The average densities of crab burrows and pneumatophores under each chamber were 3.34 ± 0.78 (i.e. $33.4 \pm 7.8 \text{ m}^{-2}$) and 5.52 ± 0.46 (i.e. $55.2 \pm 4.6 \text{ m}^{-2}$). Based on the above relationships, sediment CO₂ flux, in the absence of crab burrows and pneumatophores, was estimated as $15.4 \text{ mmol m}^{-2} \text{ d}^{-1}$ under dark conditions.

4 Discussion

4.1 Drivers of sediment CO₂ flux and surface SOC variation

Sediment water content and the proportion of silt and clay modulate both sediment CO₂ flux and surface SOC but in opposite directions in the mangrove forests. This phenomenon is mainly associated with OC oxidation pathways. Firstly, sediment water content, as a measure of sediment moisture, strongly controls organic material decay (Moyano et al., 2012) and thus is of primary importance in predicting surface SOC and sediment flux. Much of the leached dissolved organic material in mangroves is labile (Kristensen et al., 2008a) and is decayed efficiently under oxic conditions. Even cellulose and lignin can be readily degraded in oxic environments but only slowly degraded under anoxic conditions (Kristensen et al., 2008a). Further, high sediment water content corresponds to more anoxic conditions, which dampen microbial respiration. The negative impact of sediment water content on sediment respiration is consistent with the findings in a Thailand mangrove (Poungparn et al., 2009). Conversely, high sediment water content, which hampers OC oxidation, facilitates sediment C storage and thus high SOC content. Secondly, high percentages of fine-grained sediment ($<63 \mu\text{m}$) generally correlate with high OC and thus SOC stock (Bulmer et al., 2015), likely due to low levels of organic matter oxidation in the fine sediment and a hydrological regime favouring

OC deposition rather than export, as well as reducing oxygenation of the sediment. Fine-grained sediments also reduce oxygenation and thus C mineralisation rate. This inference is mirrored by the significant correlation between the proportion of fine-grained sediment and sediment volumetric water content in our study.

Both sediment CO₂ flux and surface SOC had a positive relationship with sediment Chl a. Firstly, the microphytobenthos are benthic primary producers that generally respire CO₂ under dark conditions and assimilate CO₂ through photosynthesis under light conditions (Bouillon et al., 2008). This mechanism could explain the significantly higher sediment CO₂ flux under dark conditions than light conditions. Further, our result showed that Chl a content was higher in *A. marina* (988 µg L⁻¹) than in *R. stylosa* (952 µg L⁻¹) patches, probably because of the lack of light stress in *A. marina* (Leopold et al., 2015), and contributes to the lower sediment CO₂ flux in *A. marina* than in *R. stylosa*. The positive relationship between sediment Chl a and CO₂ flux is attributed to respiration of the heterotrophic biofilms, as has been demonstrated in a study in New Zealand (Bulmer et al., 2015). Secondly, the microphytobenthos are a significant component of primary production in estuaries and shallow bays, as they can provide up to half of the total primary production and their biomass remains high even in low production locations (Davoult et al., 2009). Microphytobenthic primary production ranges between 29 and 314 g C m⁻² yr⁻¹, with variability most likely driven by irradiance and algae biomass (Underwood, 2010). It is their C production that contributes to the positive relationship between Chl a and surface SOC content observed in our study. Even though sediment Chl a also contributes to the increase of sediment CO₂ flux, this effect may be more than offset by their high contribution of C production to surface SOC content. Conversely, dense microalgal mats may serve as a physical barrier to gas diffusion and thus reduce sediment CO₂ flux (Leopold et al. 2013).

Surface SOC content varied significantly with seasons, sediment salinity, mangrove species and landform settings, in addition to the above factors. Firstly, the relatively higher surface SOC content in winter may be due to higher OC oxidation in summer than in winter, as has been found in the subtropical mangroves in southeast Queensland, Australia, and in Hong Kong, China (Allen et al., 2011; Chen et al., 2012). Different factors were proposed to drive the seasonal variation of OC oxidation, including sediment temperature and water content (Chen et al., 2012; Pongparn et al., 2009). However, in the current study, surface SOC content had a positive relationship with sediment salinity, which is higher in winter than in summer due to higher precipitation in the latter season. High salinities impede OC oxidation by microbes. Consequently, sediment salinity is likely to be predominantly

responsible for the seasonal difference in sediment OC oxidation and surface SOC content in our study. Nevertheless, the seasonal difference in sediment OC oxidation and surface SOC content could also be due to increased export during the wet season, e.g., subsurface groundwater discharge, erosion and runoff of surface organic matter. Reduced rainfall also may reduce export due to erosion resulting from river flow. Secondly, the higher surface SOC content in the *Avicennia* forest is probably due to its better adaptation to high salinities, compared with the *Rhizophora* forest. This kind of adaptation is considered to exert a positive impact on OC accumulation in sediment (Deborde et al., 2015). Although oxygen can be released through pneumatophores of *Avicennia* and promotes OC decomposition, this effect may be more than counteracted by the effect of salinities. Lastly, surface SOC content increased along the transect from creekside through mid to landward locations, supporting the expectation that infrequent inundation reduces tidal export; as has been demonstrated by findings in a Micronesian mangrove (Kauffman et al., 2011). Even though water-logging conditions, as mentioned in the context, may facilitate OC storage along the transect from creek side to landward locations, their effect may be outweighed by inundation periods, which explain more OC export at creekside than landward locations. Sediment salinity shows a parallel trend with surface SOC content, and may account for the variation of surface SOC content along the transect.

4.2 Sediment CO₂ flux without the influence of biogenic structures

Sediment CO₂ flux, if not considering the influence of crab burrows and pneumatophores, averaged at 15.4 mmol m⁻² d⁻¹ in *A. marina* forests under dark conditions. This value falls within the range of reported sediment CO₂ flux (6–241 mmol m⁻² d⁻¹), but lower than the average flux (61 mmol m⁻² d⁻¹) under dark conditions for global mangroves (Bouillon et al., 2008). When the effect of biogenic structures was considered, the increase in CO₂ flux resulting from average densities of crab burrows and pneumatophores was 2.5 and 1.6× those of CO₂ flux from the sediment–air interface, respectively, and are comparable to the increase resulting from crab burrows (1.9–4.7×) and pneumatophores (3–3.9×) in a Tanzanian mangrove (*A. marina*) forest (Kristensen et al., 2008b). The enhancement of sediment CO₂ flux by crab burrows results from the increase of gas transportation from the sediment–air interface via burrows, as well as open lenticels on pneumatophores, which promote CO₂ release from the plant and sediment (Kristensen et al., 2008b).

4.3 Interrelationships among influential factors

The density of crab burrows demonstrate positive correlations with both sediment volumetric water content and Chl a, and to vary with species and landform settings. The increase of sediment water content with the density of crab burrows in our study is in agreement with a study in Argentina, probably due to the bioturbation effect of crabs of loosening sediment structure, increasing hydraulic connectivity, porewater flow, and decreasing sediment firmness (Botto & Iribarne, 2000; Call et al., 2015; Lee, 1999). Estuarine macrobenthos, including crabs, appear to be more abundant in sediment rich in organic matter (Tolhurst et al., 2010). Isotopic analyses ($\delta^{13}\text{C}$) suggested that microphytobenthos were likely one of the food sources of crabs, although mixed C sources were possible, in a mangrove forest in southeast Queensland, Australia (Guest & Connolly, 2004). Further, crabs seem to forage (and defecate) in close proximity to their burrows (Guest & Connolly, 2004). These evidences could explain the positive correlation between the density of crab burrows and sediment Chl a. Additionally, crab burrows increase oxygenation of the sediment and thereby facilitate the decomposition of OC, releasing available CO_2 for the surface microphytobenthos and increasing [Chl a]. Crab processing of mangrove OC also accelerates nutrient recycling (Werry & Lee, 2005). Meanwhile, the change in sediment Chl a is generally in agreement with the change of burrow density along the transect from creekside to landward locations. The higher burrow density in *A. marina* than *R. stylosa* forests may be related to a preference for leaf litter among crabs. Nitrogen content was higher in the senescent leaves of *A. marina* than those of *R. stylosa* (0.65% vs 0.41%) (Werry & Lee, 2005), which may promote the use by crabs for the more nutritious leaves of *A. marina*. Further, leaves of *A. marina* have a low condensed tannin content (Zhou et al., 2010), which is relatively high in *R. stylosa* (Lin et al., 2010). High condensed tannin in *R. stylosa* leaves may deter detritivores, such as crabs. In addition, low levels of condensed tannin in *A. marina* leaves also facilitate microbial or meiofaunal colonisation (Zhou et al., 2010), which in turn increases the nutrient content of leaves and their value to crabs. Some local crab species, however, are able to utilise fresh *R. stylosa* leaves (Harada & Lee, 2016).

Sediment Chl a had a negative correlation with sediment salinity and varied with seasons and landform settings. The higher Chl a in summer than in winter is in line with another study in southeast Queensland, Australia (Dunn et al., 2012), and is probably due to the high photosynthesis of microphytobenthos in summer than in winter. The negative impact of sediment salinity on Chl a may be attributable to the downward motility of microphytobenthos under the elevated salinity (Underwood, 2002), while Chl a measurement was focused on the upper 1 cm of biofilm in our study. The significantly higher Chl a in mid

mangroves than other locations is likely a reflection of shading, which is highest in the flourishing mid forests. The increase in shading is claimed to give rise to microphytobenthic populations (Tolhurst et al., 2010), due to avoidance of photo-inhibition.

This study provides clues on facilitating blue C management from the perspective of SOC content and CO₂ efflux. Initiatives on mangrove restoration and rehabilitation should be cautious when habitats are dominated by high proportions of coarse particles (e.g. sand and gravels), which promote sediment CO₂ efflux and hamper SOC storage, as does low sediment water content. Sediment surface microphytobenthos may enhance both SOC content and CO₂ efflux, and is neutral to blue C management. Future studies are expected to involve more belowground processes in the structural equation modelling, such as decomposition of roots and leaf litter.

Data availability

Data are available upon request (oyxiaoguang@gmail.com).

Acknowledgements

We thank Ryan Stuart and Jeremy Carrington (Griffith University) for their assistance with the muffle furnace. We appreciate the critical comments from the anonymous referee on the ms.

References

- Adame, M.F., Kauffman, J.B., Medina, I., Gamboa, J.N., Torres, O., Caamal, J.P., Reza, M., & Herrera-Silveira, J.A. (2013). Carbon stocks of tropical coastal wetlands within the karstic landscape of the Mexican Caribbean. *PLoS One*, *8*, e56569.
- Allen, D., Dalal, R.C., Rennenberg, H., & Schmidt, S. (2011). Seasonal variation in nitrous oxide and methane emissions from subtropical estuary and coastal mangrove sediments, Australia. *Plant Biology (Stuttg)*, *13*, 126-133. doi: 10.1111/j.1438-8677.2010.00331.x.
- Alongi, D.M. (2014). Carbon cycling and storage in mangrove forests. *Annu. Rev. Mar. Sci.*, *6*, 195-219.
- Botto, F., & Iribarne, O. (2000). Contrasting effects of two burrowing crabs (*Chasmagnathus granulata* and *Uca uruguayensis*) on sediment composition and transport in estuarine environments. *Estuar. Coast. Shelf S.*, *51*, 141-151. doi: 10.1006/ecss.2000.0642.

- Bouillon, S., Borges, A.V., Castañeda-Moya, E., Diele, K., Dittmar, T., Duke, N.C., Kristensen, E., Lee, S.Y., Marchand, C., Middelburg, J.J., Rivera-Monroy, V.H., Smith III, T.J., & Twilley, R.R. (2008). Mangrove production and carbon sinks: a revision of global budget estimates. *Global Biogeochem. Cy.*, 22, GB2013.
- Brito, A., Newton, A., Tett, P., & Fernandes, T. (2009). Development of an optimal methodology for the extraction of microphytobenthic chlorophyll. *Journal of International Environmental Application and Science*, 42-54.
- Brown, D.R., Conrad, S., Akkerman, K., Fairfax, S., Fredericks, J., Hanrio, E., Sanders, L.M., Scott, E., Skillington, A., Tucker, J., van Santen, M.L., & Sanders, C.J. (2016). Seagrass, mangrove and saltmarsh sedimentary carbon stocks in an urban estuary; Coffs Harbour, Australia. *Regional Studies in Marine Science*, 8, Part 1, 1-6. doi: <http://dx.doi.org/10.1016/j.rsma.2016.08.005>.
- Bulmer, R., Lundquist, C., & Schwendenmann, L. (2015). Sediment properties and CO₂ efflux from intact and cleared temperate mangrove forests. *Biogeosciences*, 12, 6169-6180. doi: 10.5194/bg-12-6169-2015.
- Call, M., Maher, D.T., Santos, I.R., Ruiz-Halpern, S., Mangion, P., Sanders, C.J., Erler, D.V., Oakes, J.M., Rosentreter, J., Murray, R., & Eyre, B.D. (2015). Spatial and temporal variability of carbon dioxide and methane fluxes over semi-diurnal and spring-neap-spring timescales in a mangrove creek. *Geochim. Cosmochim. Acta*, 150, 211-225.
- Cerón-Bretón, J.G., Cerón-Bretón, R.M., Guerra-Santos, J.J., & Córdova-Quiroz, A.V. (2014). Estimation of regional carbon storage potential in mangrove soils on Carmen Island, Campeche, Mexico. In C. d. R. V. Morgado & V. P. P. Esteves (Eds.), *CO₂ Sequestration and Valorization*: inTech.
- Chen, G.C., Tam, N.F.Y., & Ye, Y. (2010). Summer fluxes of atmospheric greenhouse gases N₂O, CH₄ and CO₂ from mangrove soil in South China. *Sci. Total Environ.*, 408, 2761-2767. doi: 10.1016/j.scitotenv.2010.03.007.
- Chen, G.C., Tam, N.F.Y., & Ye, Y. (2012). Spatial and seasonal variations of atmospheric N₂O and CO₂ fluxes from a subtropical mangrove swamp and their relationships with soil characteristics. *Soil Biol. Biochem.*, 48, 175-181. doi: 10.1016/j.soilbio.2012.01.029.
- Davoult, D., Migné, A., Créach, A., Gevaert, F., Hubas, C., Spilmont, N., & Boucher, G. (2009). Spatio-temporal variability of intertidal benthic primary production and respiration in the western part of the Mont Saint-Michel Bay (western English Channel, France). *Hydrobiologia*, 620, 163-172.

- Deborde, J., Marchand, C., Molnar, N., Patrona, L.D., & Meziane, T. (2015). Concentrations and fractionation of carbon, iron, sulfur, nitrogen and phosphorus in mangrove sediments along an intertidal gradient (semi-arid climate, New Caledonia). *Journal of Marine Science and Engineering*, 3, 52-72.
- Donato, D.C., Kauffman, J.B., Murdiyarso, D., Kumianto, S., Stidham, M., & Kanninen, M. (2011). Mangroves among the most carbon-rich forests in the tropics. *Nat. Geosci.*, 4, 293-297.
- Douglas, D., & McConchie, D. (1994). *Analytical sedimentology*. London, UK: Chapman and Hall.
- Dunn, R.J.K., Welsh, D.T., Jordan, M.A., Waltham, N.J., Lemckert, C.J., & Teasdale, P.R. (2012). Benthic metabolism and nitrogen dynamics in a sub-tropical coastal lagoon: microphytobenthos stimulate nitrification and nitrate reduction through photosynthetic oxygen evolution. *Estuar. Coast. Shelf S.*, 113, 272-282. doi: 10.1016/j.ecss.2012.08.016.
- Epskamp, S. (2014). semPlot: Path diagrams and visual analysis of various SEM packages' output. R package version 1.0.1. Retrieved from <https://CRAN.R-project.org/package=semPlot>
- Fox, J., & Weisberg, S. (2011). *An {R} Companion to Applied Regression*, second ed. Thousand Oaks CA: Sage. Retrieved from <http://socserv.socsci.mcmaster.ca/jfox/Books/Companion>
- Friess, D., Richards, D., & Phang, V.H. (2015). Mangrove forests store high densities of carbon across the tropical urban landscape of Singapore. *Urban Ecosystems*, 19, 795-810. doi: 10.1007/s11252-015-0511-3.
- Guest, M.A., & Connolly, R.M. (2004). Fine-scale movement and assimilation of carbon in saltmarsh and mangrove habitat by resident animals. *Aquat. Ecol.*, 38, 599-609.
- Harada, Y., & Lee, S.Y. (2016). Foraging behavior of the mangrove sesarmid crab *Neosarmatium trispinosum* enhances food intake and nutrient retention in a low-quality food environment. *Estuar. Coast. Shelf S.*, 174, 41-48.
- Hoyle, R.H. (2012). *Handbook of Structural Equation Modeling*. New York, USA: Guilford Press.
- Jensen, L.S., Mueller, T., Tate, K.R., Ross, D.J., Magid, J., & Nielsen, N.E. (1996). Soil surface CO₂ flux as an index of soil respiration in situ: a comparison of two chamber methods. *Soil Biol. Biochem.*, 28, 1297-1306.

- Kabwe, L.K., Hendry, M.J., Wilson, G.W., & Lawrence, J.R. (2002). Quantifying CO₂ fluxes from soil surfaces to the atmosphere. *J. Hydrol.*, *260*, 1-14.
- Kauffman, J.B., Heider, C., Cole, T.G., Dwire, K.A., & Donato, D.C. (2011). Ecosystem carbon stocks of Micronesian mangrove forests. *Wetlands*, *31*, 343-352.
- Korkmaz S, Goksuluk D, & G., Z. (2014). MVN: an R package for assessing multivariate normality. *The R Journal*, *6*, 151-162.
- Kristensen, E., & Alongi, D.M. (2006). Control by fiddler crabs (*Uca vocans*) and plant roots (*Avicennia marina*) on carbon, iron, and sulfur biogeochemistry in mangrove sediment. *Limnol. Oceanogr.*, *51*, 1557-1571.
- Kristensen, E., Bouillon, S., Dittmar, T., & Marchand, C. (2008a). Organic carbon dynamics in mangrove ecosystems: a review. *Aquat. Bot.*, *89*, 201-219. doi: 10.1016/j.aquabot.2007.12.005.
- Kristensen, E., Flindt, M.R., Ulomi, S., Borges, A.V., Abril, G., & Bouillon, S. (2008b). Emission of CO₂ and CH₄ to the atmosphere by sediments and open waters in two Tanzanian mangrove forests. *Mar. Ecol. Prog. Ser.*, *370*, 53-67. doi: 10.3354/meps07642.
- Lee, S.Y. (1999). Tropical mangrove ecology: physical and biotic factors influencing ecosystem structure and function. *Aust. J. Ecol.*, *24*, 355-366.
- Lee, S.Y. (2008). Mangrove macrobenthos: assemblages, services, and linkages. *J. Sea Res.*, *59*, 16-29. doi: 10.1016/j.seares.2007.05.002.
- Leopold, A., Marchand, C., Deborde, J., & Allenbach, M. (2015). Temporal variability of CO₂ fluxes at the sediment-air interface in mangroves (New Caledonia). *Sci. Total Environ.*, *502*, 617-626.
- Leopold, A., Marchand, C., Deborde, J., Chaduteau, C., & Allenbach, M. (2013). Influence of mangrove zonation on CO₂ fluxes at the sediment-air interface (New Caledonia). *Geoderma*, *202*, 62-70.
- Lin, Y.-M., Liu, X.-W., Zhang, H., Fan, H.-Q., & Lin, G.-H. (2010). Nutrient conservation strategies of a mangrove species *Rhizophora stylosa* under nutrient limitation. *Plant Soil*, *326*, 469-479. doi: 10.1007/s11104-009-0026-x.
- Mcleod, E., Chmura, G.L., Bouillon, S., Salm, R., Björk, M., Duarte, C.M., Lovelock, C.E., Schlesinger, W.H., & Silliman, B.R. (2011). A blueprint for blue carbon: toward an improved understanding of the role of vegetated coastal habitats in sequestering CO₂. *Front. Ecol. Environ.*, *9*, 552-560.

- Moyano, F.E., Vasilyeva, N., Bouckaert, L., Cook, F., Craine, J., Curiel Yuste, J., Don, A., Epron, D., Formanek, P., Franzluebbers, A., Ilstedt, U., Kätterer, T., Orchard, V., Reichstein, M., Rey, A., Ruamps, L., Subke, J.A., Thomsen, I.K., & Chenu, C. (2012). The moisture response of soil heterotrophic respiration: interaction with soil properties. *Biogeosciences*, *9*, 1173-1182. doi: 10.5194/bg-9-1173-2012.
- Penha-Lopes, G., Kristensen, E., Flindt, M., Mangion, P., Bouillon, S., & Paula, J. (2010). The role of biogenic structures on the biogeochemical functioning of mangrove constructed wetlands sediments—a mesocosm approach. *Mar. Pollut. Bull.*, *60*, 560-572.
- Poungparn, S., Komiyama, A., Tanaka, A., Sangtjean, T., Maknual, C., Kato, S., Tanapermpool, P., & Patanaponpaiboon, P. (2009). Carbon dioxide emission through soil respiration in a secondary mangrove forest of eastern Thailand. *J. Trop. Ecol.*, *25*, 393-400. doi: 10.1017/S0266467409006154.
- PP Systems (2012). SBA-5 CO₂ Analyzer Operation Manual Version 1.05. PP Systems Inc., USA
- Quinn, G.P., & Keough, M.J. (2002). *Experimental Design and Data Analysis for Biologists*. Cambridge, UK: Cambridge University Press.
- R Core Team (2014). A Language and Environment for Statistical Computing, R Foundation for Statistical Computing. Vienna, Austria. available at: <http://www.R-project.org/>.
- Revelle, W. (2015). psych: Procedures for personality and psychological research, Northwestern University, Evanston, Illinois, USA. Retrieved from <http://CRAN.R-project.org/package=psych> (Version = 15.8).
- Rosseel, Y. (2012). lavaan: an R package for structural equation modeling. *J. Stat. Softw.*, *48*, 1-36.
- Schumacher, B. (2002). *Methods for the Determination of Total Organic Carbon (TOC) in Soils and Sediments*. Washington, DC, USA: Ecological Risk Assessment Support Center, Office of Research and Development. US Environmental Protection Agency.
- Schumacker, R.E., & Lomax, R.G. (2004). *A Beginner's Guide to Structural Equation Modeling*. New York, USA: Psychology Press.
- Tolhurst, T., Defew, E., & Dye, A. (2010). Lack of correlation between surface macrofauna, meiofauna, erosion threshold and biogeochemical properties of sediments within an intertidal mudflat and mangrove forest. *Hydrobiologia*, *652*, 1-13.

- Underwood, G.J.C. (2002). Adaptations of tropical marine microphytobenthic assemblages along a gradient of light and nutrient availability in Suva Lagoon, Fiji. *Eur. J. Phycol.*, 37, 449-462.
- Underwood, G.J.C. (2010). Microphytobenthos and phytoplankton in the Severn estuary, UK: Present situation and possible consequences of a tidal energy barrage. *Mar. Pollut. Bull.*, 61, 83-91. doi: 10.1016/j.marpolbul.2009.12.015.
- Werry, J., & Lee, S.Y. (2005). Grapsid crabs mediate link between mangrove litter production and estuarine planktonic food chains. *Mar. Ecol. Prog. Ser.*, 293, 165-176.
- Zhou, H.-C., Wei, S.-D., Zeng, Q., Zhang, L.-H., Tam, N.F.-y., & Lin, Y.-M. (2010). Nutrient and caloric dynamics in *Avicennia marina* leaves at different developmental and decay stages in Zhangjiang River estuary, China. *Estuar. Coast. Shelf S.*, 87, 21-26.